Ultra Scientist Vol. 28(2)A, 91-110 (2016). ISSN 2231-3478 (Print)
www.ultrascientist.org 2319-8052 (Online)

Influence of Slip and Joule Heating on MHD Peristaltic Blood flow with uniform Porous medium through an Inclined asymmetric Vertical Tapered Channel in the presence of Radiation-Blood flow model

Sk. ABZAL[*1], S.VIJAYA KUMAR VARMA[2] and S.RAVI KUMAR[3]

[1]Department of Mathematics, NBKR Institute of Science and Technology (Autonomous), Vidyanagar, SPSR Nellore,Andhra Pradesh (India).
[2]Department of Mathematics, Sri Venkateswara University, Tirupati, Andhra Pradesh (India).
[3]Department of Mathematics NBKR Institute of Science and Technology (Autonomous), Vidyanagar, SPSR Nellore,Andhra Pradesh (India).
Corresponding author email:abbuoct23@gmail.com

(Acceptance Date 15th June, 2016)

Abstract

In this article, an influence of slip and joule heating on MHD peristaltic blood flow with uniform porous medium through an inclined asymmetric vertical tapered channel in the presence of radiation -blood flow model have been investigated. The impact of all the physical parameters is plotted for velocity profile, pressure gradient, temperature and heat transfer coefficient. It is notice that the axial velocity increases with increase in M, β, η and α. We observe that the pressure gradient enhances with increase in M, β, η and α. However reverse situation is observed for an increase in the values of porous parameter (Da) and Volumetric flow rate (Q). Further, we notice that the temperature distribution increases with increase in M, Pr, Da, N, γ and Br and also temperature distribution decreases with increase in β and η.

Key words: MHD, Joule heating, radiation, porous medium and Inclined channel.

1. Introduction

To the best of our knowledge, no investigation has been made yet to analyze an influence of slip and joule heating on MHD peristaltic blood flow through an inclined asymmetric vertical tapered channel in the

presence of radiation effect-blood flow model. The purpose of the present paper is to provide such an attempt for a MHD Newtonian fluid through porous medium with Joule heating and radiation under the influence of slip conditions. Interest in peristaltic flow has been aroused by its relevance to biological processes, and its potential for industrial and medical applications. The behaviour of most of the physiological fluids, oil, hydrocarbons and polymer are known to be non-Newtonian. One of the major chemical mechanisms for fluid transport in many biological systems is well known to physiologists to be peristalsis. Peristalsis is an important mechanism for mixing and transporting fluids, which is generated by a progressive wave of contraction or expansion moving along a tube. This travelling wave phenomenon is referred to as peristalsis. Peristalsis has its immense applications in medical physiology as well as in industry. In medical physiology, it is involved in the motion of food material in the GIT. In reproductive parts, it helps in the transportation of spermatozoa in the ductus efferentes of the male reproductive tract and in the cervical canal, in the embryo implantation in the fundus site of female uterus and in the movement of an ovum in the fallopian tubes of the female reproductive parts. It also helps in the vasomotion of small blood vessels as well as blood flow in arteries, transport of urine from a kidney to ureter and movement of secretions in glandular ducts (bile and saliva). Some worms also move with the help of peristalsis. Nowadays, peristalsis has exploited its significance in industry, like in sanitary fluid transport, artificial blood pumps in the heart-lung machine and transport of corrosive fluids where the contact of the fluid with the boundary is prohibited. Peristaltic studies are useful for having a proper understanding of the functioning of different machines used by clinicians for pumping blood and magnetic resonance imaging (MRI). The study of the mechanisms of peristalsis, in both mechanical and physiological situations, has been the object of scientific research for quite some time. Several theoretical and experimental attempts have been done in Latham[12] to find out the peristaltic action in different situations. Mathematical studies of peristalsis were initiated by Fung & Yih[3], Shapiro *et al*.[25], and others. Most of these analyses are based on Navier-Stokes equation, considering flow in a circular cylindrical tube or two-dimensional channel with a sinusoidal displacement wave travelling in its wall at a constant velocity. Influence of velocity slip conditions on MHD peristaltic flow of a Prandtl fluid in anon-uniform channel was discussed by Kumar *et al.*[11]. In another attempt, T. Hayat *et al*.[5] studied on an influence of convective conditions in radiative peristaltic flow of pseudo plastic nanofluid in a tapered asymmetric channel. Peristaltic Transport in a Slip Flow has been discussed by Kawang-Hua Chu, W., and Fang, J[7]. In another paper, A.V. Ramana Kumari and G. Radhakrishnamacharya[17] discussed on Effect of slip on peristaltic transport in an inclined channel with wall effects. Afterward, few relevant interested discussions can be seen via attempts such as R.H. Reddy *et al*.[24], Srinivas, S. *et al*.[27], S.V.H.N. Krishna Kumari *et al*.[10], Lika Hummady *et al*.[13], Ravikumar[19-23], T. Hayat, M.U. Qureshi and N.Ali[6], M. Mishra, A. R. Rao[14].

Heat transfer analysis is prevalent in the study of peristaltic flows due to its large

number of applications in processes like hemodialysis (the method used for removing waste products from blood in the case of renal failure of a kidney) and oxygenation. Bioheat is currently considered as heat transfer in the human body. In view of thermotherapy (application of heat to the body for treatment, examples pain relief, increase of blood flow and others) and human thermoregulation system (ability of living body to maintain body temperature within certain limits in case of surrounding temperature variations) as mentioned by Srinivas and Kothandapani[9], bioheat transfer has attracted many biomedical experts. Heat transfer analysis is important especially in the case of non-Newtonian peristaltic rheology as there involve many intricate processes like heat conduction in tissues, heat transfer during perfusion (process of delivery of blood to capillary bed) of arterial-venous blood, metabolic heat generation and heat transfer due to some external interactions like mobile phones and radioactive treatments. It is also helpful in the treatment of diseases like the removal of undesirable tissues in cancer. Vajravelu *et al*.[28] have presented a mathematical model for peristaltic flow and heat transfer in a vertical porous annulus with long wave approximation. In another attempt, Nadeem *et al*.[16] discussed on influence of heat transfer in peristalsis with variable viscosity. Sabir Ali Shehzad *et al*.[26] investigated on MHD Mixed Convective Peristaltic Motion of Nanofluid with Joule Heating and Thermophoresis Effects. T.Hayat *et al*.[4] studied on Soret and Dufour effects on peristaltic flow in an asymmetric channel. Mustafa, M[15] has been investigated on mixed convective peristaltic flow of fourth grade fluid with Dufour and Soret effects. Recently, Ravi Kumar[18] investigated on Analysis of Heat Transfer on MHD Peristaltic Blood Flow with Porous Medium through Coaxial Vertical Tapered Asymmetric Channel with Radiation – Blood Flow Study. Some pertinent studies on the present topic can be found from the list of Refs. Such as K. Venugopal Reddy *et al*.[29], M Kothandapani *et al*.[8], Sk Abzal *et al*.[1]

2. Formulation of the problem :

The model simulates the peristaltic transport of a viscous fluid through an infinite two-dimensional asymmetric vertical tapered channel through the porous medium. Asymmetry in the flow is due to the propagation of peristaltic waves of different amplitudes and phase on the channel walls. We assume that the fluid is subject to a constant transverse magnetic field B_0. The flow is generated by sinusoidal wave trains propagating with steady speed c along the tapered asymmetric channel walls[6,20-22].

The geometry of the wall surface is defined as

$$Y = H_2 = b + m'X + d\sin\left[\frac{2\pi}{\lambda}(X - ct)\right] \quad (1)$$

$$Y = H_1 = -b - m'X - d\sin\left[\frac{2\pi}{\lambda}(X - ct) + \phi\right] \quad (2)$$

Where b is the half-width of the channel, d is the wave amplitude, c is the phase speed of the wave and m' $(m' << 1)$ is the non-uniform parameter, λ is the wavelength, t is the time and X is the direction of wave propagation. The phase difference ϕ varies in the range $0 \le \phi \le \pi$, $\phi = 0$ corresponds to symmetric channel with waves out of phase and further b, d and ϕ satisfy the following conditions for the divergent channel at the inlet

$$d\cos(\frac{\phi}{2}) \le b$$

It is assumed that the left wall of the channel is maintained at temperature T_0 while the right wall has temperature T_1.

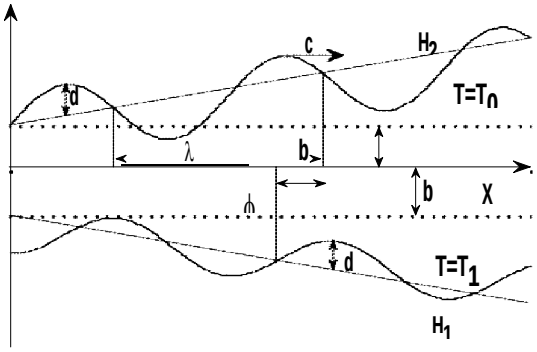

Fig. 1 Schematic diagram of the physical model

The equations governing the motion for the present problem prescribed by
The continuity equation is

$$\frac{\partial u}{\partial x}+\frac{\partial v}{\partial y}=0 \qquad (3)$$

The movement equations are

$$\rho\left[u\frac{\partial u}{\partial x}+v\frac{\partial u}{\partial y}\right]=-\frac{\partial p}{\partial x}+\mu\left[\frac{\partial^2 u}{\partial x^2}+\frac{\partial^2 u}{\partial y^2}\right]-$$

$$\left[\sigma B_0^{\,2}\right](u+c)-\left[\frac{\mu}{k_1}\right](u+c)+\rho g\sin\alpha \qquad (4)$$

$$\rho\left[u\frac{\partial v}{\partial x}+v\frac{\partial v}{\partial y}\right]=-\frac{\partial p}{\partial y}+\mu\left[\frac{\partial^2 v}{\partial x^2}+\frac{\partial^2 v}{\partial y^2}\right]-$$

$$\left[\sigma B_0^{\,2}\right]v-\left[\frac{\mu}{k_1}\right]v-\rho g\cos\alpha \qquad (5)$$

The energy equation is

$$\rho C_p\left[u\frac{\partial}{\partial x}+v\frac{\partial}{\partial y}\right]T=k\left[\frac{\partial^2}{\partial x^2}+\frac{\partial^2}{\partial y^2}\right]T+$$

$$Q_0+\sigma B_0^{\,2}u^2-\frac{\partial q}{\partial y} \qquad (6)$$

u and v are the velocity components in the corresponding coordinates, k_1 is the permeability of the porous medium, ρ is the density of the fluid, p is the fluid pressure, k is the thermal conductivity, μ is the coefficient of the viscosity, Q_0 is the constant heat addition/ absorption, C_p is the specific heat at constant pressure, σ is the electrical conductivity, g is the acceleration due to gravity and T is the temperature of the fluid.
The relative boundary conditions are

$$\bar{U}=0,\quad \bar{T}=T_0 \quad \text{at} \quad \bar{Y}=\bar{H}_1$$

$$\bar{U}=0,\quad \bar{T}=T_1 \quad \text{at} \quad \bar{Y}=\bar{H}_2$$

The radioactive heat flux (Cogley *et al.*[2]) is given by

$$\frac{\partial q}{\partial y}=4\alpha^2(T_0-T_1) \qquad (7)$$

here α is the mean radiation absorption coefficient.
Introducing a wave frame (x, y) moving with velocity c away from the fixed frame (X, Y) by the transformation
$x = X\text{-}ct$, $y = Y$, $u = U\text{-}c$, $v = V$ and
$p(x) = P(X,t)$ (8)
Introducing the following non-dimensional quantities:

$$\bar{x}=\frac{x}{\lambda}\ \ \bar{y}=\frac{y}{b}\ \ \bar{t}=\frac{ct}{\lambda}\ \ \bar{u}=\frac{u}{c}\ \ \bar{v}=\frac{v}{c\delta}\ \ h_1=\frac{H_1}{b}$$

$$h_2=\frac{H_2}{b}\quad p=\frac{b^2 p}{c\,\lambda\,\mu}\quad \theta=\frac{T-T_0}{T_1-T_0}\quad \delta=\frac{b}{\lambda}$$

$$\text{Re} = \frac{\rho c b}{\mu} \quad N^2 = \frac{4\alpha^2 d_1^2}{k} \quad \varepsilon = \frac{d}{b} \quad \eta = \frac{\rho a_0^2 g}{\mu c}$$

$$\eta_1 = \frac{\rho a_0^3 g}{\lambda \mu c} \tag{9}$$

where $\varepsilon = \frac{d}{b}$ is the non-dimensional amplitude of channel $\delta = \frac{b}{\lambda}$, is the wave number, $k_1 = \frac{\lambda m'}{b}$ is the non - uniform parameter, Re is the Reynolds number, M is the Hartman number, $K = \frac{k}{b^2}$ Permeability parameter, Pr is the Prandtl number, E_c is the Eckert number, γ is the heat source/sink parameter, B_r (= $E_c P_r$) is the Brinkman number, η and η_1 are gravitational parameters and N^2 is the radiation parameter.

3. Solution of the problem :

In view of the above transformations (8) and non-dimensional variables (9), equations (3-6) are reduced to the following non-dimensional form after dropping the bars

$$\text{Re}\,\delta\left[u\frac{\partial u}{\partial x} + v\frac{\partial u}{\partial y}\right] =$$

$$\left(-\frac{\partial p}{\partial x} + \delta^2\frac{\partial^2 u}{\partial x^2} + \frac{\partial^2 u}{\partial y^2} - Au - A + \eta\sin\alpha\right) \tag{10}$$

$$\text{Re}\,\delta^3\left[u\frac{\partial v}{\partial x} + v\frac{\partial v}{\partial y}\right] = \left(-\frac{\partial p}{\partial y} + \delta^4\frac{\partial^2 v}{\partial x^2} + \delta^2\frac{\partial^2 v}{\partial y^2} - M^2\delta^2 v - \delta^2\frac{1}{Da}v - \eta_1\cos\alpha\right) \tag{11}$$

$$\text{Re}\left[\delta u\frac{\partial\theta}{\partial x} + v\delta\frac{\partial\theta}{\partial y}\right] = \frac{1}{\text{Pr}}\left[\delta^2\frac{\partial^2\theta}{\partial x^2} + \frac{\partial^2\theta}{\partial y^2}\right] + \beta + M^2 E u^2 + \frac{N^2\theta}{P_r} \tag{12}$$

Applying long wave length approximation and neglecting the wave number along with low-Reynolds numbers. Equations (10-12) become

$$\frac{\partial^2 u}{\partial y^2} - Au = \frac{\partial p}{\partial x} + A - \eta\sin\alpha \tag{13}$$

$$\frac{\partial p}{\partial y} = 0 \tag{14}$$

$$\frac{1}{\text{Pr}}\left[\frac{\partial^2\theta}{\partial y^2}\right] + \beta + M^2 E u^2 + \frac{N^2\theta}{P_r} = 0 \tag{15}$$

Where $A = \left(M^2 + \frac{1}{Da}\right)$

The relative boundary conditions in dimensionless form are given by

$$u = -\beta\frac{\partial u}{\partial y},\ \theta = 0 \text{ at } y = h_1 \tag{16}$$

$$u = \beta\frac{\partial u}{\partial y},\quad \theta = 1 \text{ at } y = h_2 \tag{17}$$

Where

$$h_1 = -1 - k_1 x - \varepsilon\sin\left[2\pi(x - t) + \phi\right]$$

$$h_2 = 1 + k_1 x + \varepsilon\sin\left[2\pi(x - t)\right]$$

Where β is the non-dimensional slip velocity parameter.

The solutions of velocity and temperature with

subject to boundary conditions (16) and (17) are given by

$$u = GSin\,h[\alpha\, y] + H\,Cos\,h[\alpha\, y] + F \qquad (18)$$

Where

$$\alpha = \sqrt{\left(M^2 + \frac{1}{Da}\right)}$$

$$F = \frac{D}{M^2 D + 1}\left(\eta\, Sin\alpha - \frac{\partial p}{\partial x}\right) - 1$$

$$G = \left(\frac{-F\left(\frac{a_1}{a_2}\right)(Cos\,h[\alpha\, h_1] + \beta\,\alpha\, Sin\,h[\alpha\, h_1]) - F}{Sin\,h[\alpha\, h_1] + \beta\,\alpha\, Cos\,h[\alpha\, h_1]}\right)$$

$$H = \left(\frac{F\, a_1}{a_2}\right)$$

$$a_1 = \left(\left(\frac{Sin\,h[\alpha\, h_2] - \beta\,\alpha\, Cos\,h[\alpha\, h_2]}{Sin\,h[\alpha\, h_1] + \beta\,\alpha\, Cos\,h[\alpha\, h_1]}\right) - 1\right)$$

$$a_2 = -\left(\frac{Cos\,h[\alpha\, h_1] + \beta\,\alpha\, Sin\,h[\alpha\, h_1]}{Sin\,h[\alpha\, h_1] + \beta\,\alpha\, Cos\,h[\alpha\, h_1]}\right) * (Sin\,h[\alpha\, h_2] - \beta\,\alpha\, Cos\,h[\alpha\, h_2]) + (Cos\,h[\alpha\, h_2] - \beta\,\alpha\, Sin\,h[\alpha\, h_2])$$

$$\theta = JCos[Ny] + KSin[Ny] - \left(\frac{P_r\gamma}{N^2}\right) - \left(\frac{M^2 B_r a_3}{4\alpha^2 + N^2} e^{2\alpha y}\right) - \left(\frac{M^2 B_r a_4}{4\alpha^2 + N^2} e^{-2\alpha y}\right) - \left(\frac{M^2 B_r a_5}{\alpha^2 + N^2} e^{\alpha y}\right) - \left(\frac{M^2 B_r a_6}{\alpha^2 + N^2} e^{-\alpha y}\right) - \left(\frac{M^2 B_r a_7}{N^2}\right)$$

Where

$$J = \frac{-KSin[N\,h_1] + \left(\frac{P_r\,\gamma}{N^2}\right) + \left(\frac{M^2 B_r a_3}{4\alpha^2 + N^2} e^{2\alpha h_1}\right)}{\cos[N\,h_1]} + \frac{\left(\frac{M^2 B_r a_4}{4\alpha^2 + N^2} e^{-2\alpha h_1}\right) + \left(\frac{M^2 B_r a_5}{\alpha^2 + N^2} e^{\alpha h_1}\right)}{\cos[N\,h_1]} + \frac{\left(\frac{M^2 B_r a_6}{\alpha^2 + N^2} e^{-\alpha h_1}\right) + \left(\frac{M^2 B_r a_7}{N^2}\right)}{\cos[N\,h_1]}$$

$$K = \left(\frac{-\left(\frac{P_r\,\gamma}{N^2}\right)(\cos[N\,h_1] - \cos[N\,h_2])}{Sin[N\,h_1]\cos[N\,h_2] - Sin[N\,h_2]\cos[N\,h_1]}\right) - \left(\frac{\frac{M^2 B_r a_3}{4\alpha^2 + N^2}\left(e^{2\alpha h_2}\cos[N\,h_1] - e^{2\alpha h_1}\cos[N\,h_2]\right)}{Sin[N\,h_1]\cos[N\,h_2] - Sin[N\,h_2]\cos[N\,h_1]}\right) - \left(\frac{\frac{M^2 B_r a_4}{4\alpha^2 + N^2}\left(e^{-2\alpha h_2}\cos[N\,h_1] - e^{-2\alpha h_1}\cos[N\,h_2]\right)}{Sin[N\,h_1]\cos[N\,h_2] - Sin[N\,h_2]\cos[N\,h_1]}\right) - \left(\frac{\frac{M^2 B_r a_5}{\alpha^2 + N^2}\left(e^{\alpha h_2}\cos[N\,h_1] - e^{\alpha h_1}\cos[N\,h_2]\right)}{Sin[N\,h_1]\cos[N\,h_2] - Sin[N\,h_2]\cos[N\,h_1]}\right) - \left(\frac{\frac{M^2 B_r a_6}{\alpha^2 + N^2}\left(e^{-\alpha h_2}\cos[N\,h_1] - e^{-\alpha h_1}\cos[N\,h_2]\right)}{Sin[N\,h_1]\cos[N\,h_2] - Sin[N\,h_2]\cos[N\,h_1]}\right) - \left(\frac{\frac{M^2 B_r a_7}{N^2}(\cos[N\,h_1] - \cos[N\,h_2])}{Sin[N\,h_1]\cos[N\,h_2] - Sin[N\,h_2]\cos[N\,h_1]}\right) -$$

$$\left(\frac{\cos\left[N\,h_1\right]}{Sin\left[N\,h_1\right]\cos\left[N\,h_2\right]-Sin\left[N\,h_2\right]\cos\left[N\,h_1\right]}\right)$$

$$a_3=\left(\frac{G^2}{4}+\frac{H^2}{4}+\frac{GH}{2}\right)\ a_4=\left(\frac{G^2}{4}+\frac{H^2}{4}-\frac{GH}{2}\right)$$

$$a_5=F\left(G+H\right)\ a_6=F\left(H-G\right)$$

$$a_7=\left(\frac{-G^2}{2}+\frac{H^2}{2}+F^2\right)$$

The coefficients of the heat transfer Zh_1 and Zh_2 at the walls $y = h_1$ and $y = h_2$ respectively, are given by

$$Zh_1=\theta_y h_{1x} \tag{20}$$

$$Zh_2=\theta_y h_{2x} \tag{21}$$

The solutions of the coefficient of heat transfer at $y = h_1$ and $y = h_2$ are given by

$$Zh_1=\theta_y h_{1x}=$$

$$\left(-J\,N\,Sin\left[N\,y\right]+KN\,Cos\left[N\,y\right]-\left(\frac{2\alpha M^2B_ra_3}{4\alpha^2+N^2}e^{2\alpha y}\right)-\right.$$

$$\left(\frac{-2\alpha M^2B_ra_4}{4\alpha^2+N^2}e^{-2\alpha y}\right)-\left(\frac{\alpha M^2B_ra_5}{\alpha^2+N^2}e^{\alpha y}\right)+$$

$$\left.\left(\frac{\alpha M^2B_ra_6}{\alpha^2+N^2}e^{-\alpha y}\right)\right)\ \left(-2\pi\varepsilon Cos\left[2\pi\left(x-t\right)+\phi\right]-k_1\right)$$

$$Zh_2=\theta_y h_{2x}=$$

$$\left(-J\,N\,Sin\left[N\,y\right]+KN\,Cos\left[N\,y\right]-\left(\frac{2\alpha M^2B_ra_3}{4\alpha^2+N^2}e^{2\alpha y}\right)-\right.$$

$$\left(\frac{-2\alpha M^2B_ra_4}{4\alpha^2+N^2}e^{-2\alpha y}\right)-\left(\frac{\alpha M^2B_ra_5}{\alpha^2+N^2}e^{\alpha y}\right)+$$

$$\left.\left(\frac{\alpha M^2B_ra_6}{\alpha^2+N^2}e^{-\alpha y}\right)\right)\left(2\pi\varepsilon\,Cos\left[2\pi\left(-t+x\right)\right]+k_1\right)$$

The volumetric flow rate in the wave frame is defined by

$$q=\int_{h_1}^{h_2}u\,dy=$$

$$\left(\frac{G}{\alpha}\right)\left(Cos\,h\left[\alpha\,h_2\right]-Cos\,h\left[\alpha\,h_1\right]\right)+$$

$$\left(\frac{H}{\alpha}\right)\left(Sin\,h\left[\alpha\,h_2\right]-Sin\,h\left[\alpha\,h_1\right]\right)+F\left(h_2-h_1\right) \tag{24}$$

The pressure gradient obtained from equation (24) can be expressed as

$$\frac{dp}{dx}=\left(\frac{-qA}{B}\right)+\left(\eta\,Sin\alpha-A\right) \tag{25}$$

Where

$$B=\left(\frac{-1}{\alpha}\right)\left(\frac{\left(\frac{a_1}{a_2}\right)\left(Cosh\left[\alpha\,h_1\right]+\beta\,\alpha\,Sinh\left[\alpha\,h_1\right]\right)+1}{Sinh\left[\alpha\,h_1\right]+\beta\,\alpha\,Cosh\left[\alpha\,h_1\right]}\right)*$$

$$\left(Cosh\left[\alpha\,h_2\right]-Cosh\left[\alpha\,h_1\right]\right)+$$

$$\left(\frac{a_1}{\alpha\,a_2}\right)\left(Sin\,h\left[\alpha\,h_2\right]-Sin\,h\left[\alpha\,h_1\right]\right)+\left(h_2-h_1\right)$$

The instantaneous flux Q (x, t) in the laboratory frame is

$$Q=\int_{h_2}^{h_1}\left(u+1\right)dy=q-h \tag{26}$$

The average volume flow rate over one wave

period (T = λ/c) of the peristaltic wave is defined as

$$\overline{Q} = \frac{1}{T}\int_0^T Q\,dt = q + 1 + d \qquad (27)$$

From the equations (25) and (27), the pressure gradient can be expressed as

$$\frac{dp}{dx} = \left(\frac{-\left(\overline{Q} - 1 - d\right)A}{B}\right) + \left(\eta\, Sin\alpha - A\right) \qquad (28)$$

4. Discussion of the problem

The main object of this investigation has been to study an influence of slip and joule heating on MHD peristaltic blood flow with uniform porous medium through an inclined asymmetric vertical tapered channel in the presence of radiation -blood flow model. The analytical expressions for velocity distribution, pressure gradient, and temperature and heat transfer coefficient have been derived in the previous section. The numerical and computational results are discussed through the graphical illustration. **Mathematica** software is used to find out numerical results.

Influence of Hartman number on velocity distribution can be seen through Fig. 2. It was evident that the axial velocity increases with increase in M (M = 1, 1.5, 2) being fixed Da = 0.3, ϕ = π/6, α = π/6, η = 0.5, β = 0.7, ε = 0.2, k1= 0.1, x = 0.6, t = 0.4, dp/dx = 0.5. Fig. 3 illustrates the variation in an axial velocity for different values of slip parameter β (β = 0.7, 0.8, 0.9) with fixed Da = 0.3, ϕ = π/6, α = π/6, η = 0.5, M = 1, ε = 0.2, k1= 0.1, x = 0.6, t = 0.4, dp/dx = 0.5. This figure reveals that the axial velocity increases when slip parameter β increased. Fig. 4 depicts that the axial velocity distribution (u) with various values of Da (Da = 0.1, 0.2, 0.3) with fixed other parameters. It is interested to note that the axial velocity decreases with increase in porosity parameter (Da). Effect of gravitational parameter (η) on axial velocity distribution (u) shown in figure 5 with β = 0.7, Da = 0.3 ϕ = ð/6, á = ð/6, M = 1, å= 0.2, k_1= 0.1, x = 0.6, t = 0.4, dp/dx = 0.5. We observe from this graph that the axial velocity gradually increases when increase in η. Fig. 6 revals that the various values of inclined angle α (α = 0, π/6, π/3) on axial velocity distribution (u). It has been inferred that the axial velocity slowly increases by increase in α being fixed β = 0.7, Da = 0.3 ϕ = π/6, η = 0.5, M = 1, ε = 0.2, k1= 0.1, x = 0.6, t = 0.4, dp/dx =0.5. Hence, we notice that the axial velocity increases in the entire tapered channel when an increase in M, β, η and α (see fig. 2, 3, 5 and 6) and also we observe that the axial velocity decreases in the entire tapered channel when increasing in Da (see fig. 4).

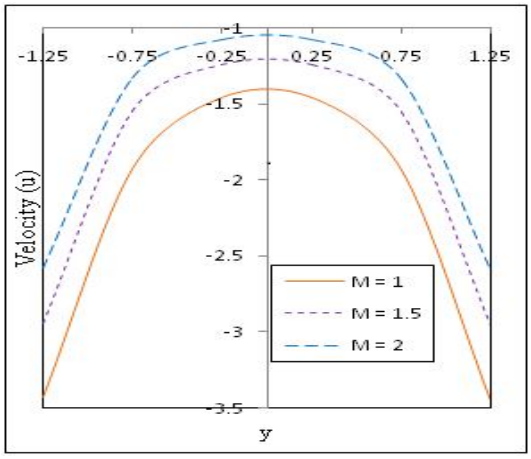

Figure (2): Velocity for different values of M with fixed Da = 0.3, ϕ = π/6, α = π/6, η = 0.5, β = 0.7, ε = 0.2, k_1= 0.1, x = 0.6, t = 0.4, dp/dx = 0.5.

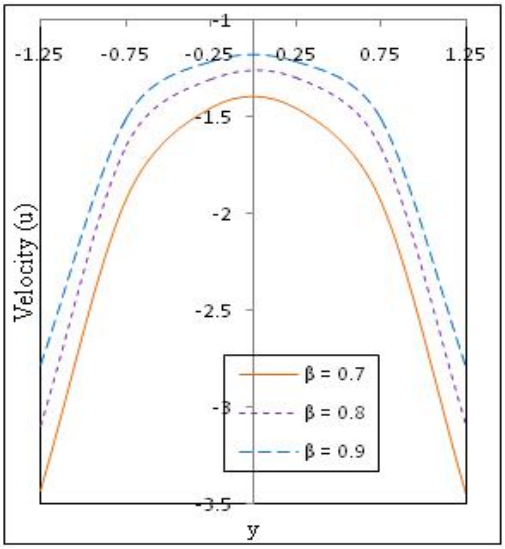

Figure (3): Velocity for different values of β with fixed Da = 0.3, ϕ = π/6, α = π/6, η = 0.5, M = 1, å= 0.2, k_1= 0.1, x = 0.6, t = 0.4, dp/dx = 0.5

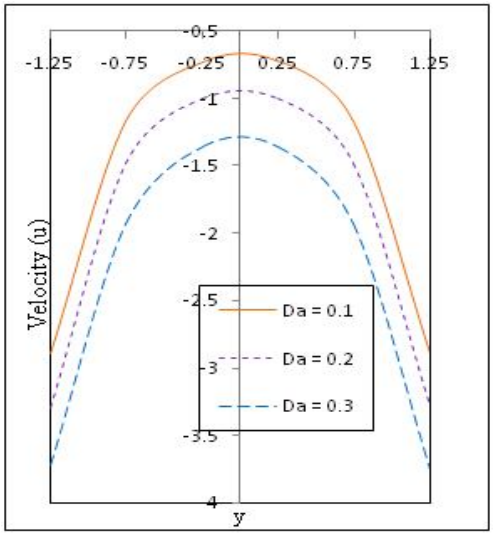

Figure (4): Velocity for different values of Da with fixed β = 0.7, ϕ = π/6, α = π/6, η = 0.5, M = 1, ε = 0.2, k_1= 0.1, x = 0.6, t = 0.4, dp/dx = 0.5.

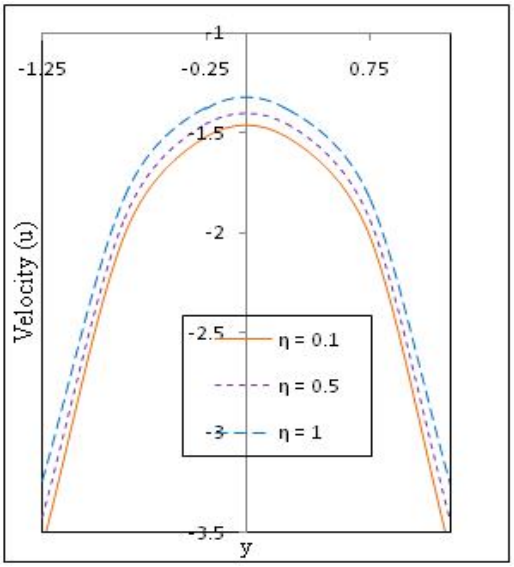

Figure (5): Velocity for different values of η with fixed β = 0.7, Da = 0.3 ϕ = π/6, α = π/6, M = 1, å= 0.2, k_1= 0.1, x = 0.6, t = 0.4, dp/dx = 0.5.

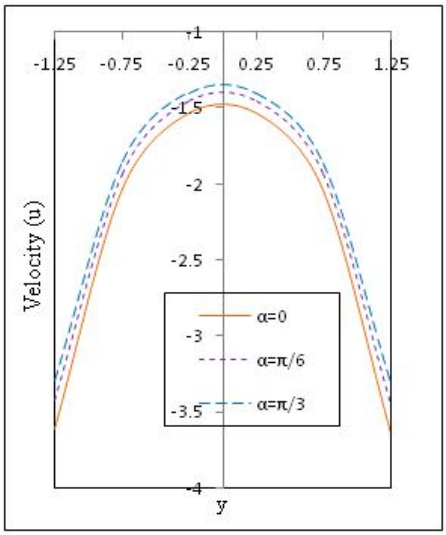

Figure (6): Velocity for different values of α with fixed β = 0.7, Da = 0.3 ϕ = π/6, η = 0.5, M = 1, ε = 0.2, k_1= 0.1, x = 0.6, t = 0.4, dp/dx = 0.5.

Fig. 7 illustrates the variation in axial pressure gradient for different values of the Hartmann number M (M = 1, 1.5, 2) with Da = 0.3, $\phi = \pi/6$, $\alpha = \pi/6$, $\eta = 0.5$, $\beta = 0.7$, $\varepsilon = 0.2$, k1= 0.1, $t = \pi/4$, $\mu = 0.2$, d = 2. This figure reveals as the values of the Hartmann number increases the magnitude of the axial pressure gradient also increases. It shows that when a strong magnetic field is applied to the flow field then higher pressure gradient is needed to pass the flow. An important result depicted in Fig. 8 that the variation in axial pressure gradient for different values of slip parameter β (β=0.7, 0.8, 0.9) with M = 1, $\phi = \pi/6$, $\alpha = \pi/6$, $\eta = 0.5$, $\varepsilon = 0.2$, k1= 0.1, $t = \pi/4$, $\overline{Q} = 0.2$, d = 2.It shows that in the wider part of channel *i.e.* x ε (0, 0.3) U (07, 1) the pressure gradient is relatively small. Hence, the flow can easily pass without imposing more pressure gradient. Similarly in the narrow part of channel *i.e.* ε (0.3, 7), the flow cannot pass easily. Therefore, it requires more pressure gradient is needed to maintain the same flux to pass through it and also we observe that the axial pressure gradient increases by the increase in β. The axial pressure gradient for different values of porous parameter Da (Da = 0.1, 0.2, 0.3) is plotted in Fig, 9. It can be seen that the axial pressure gradient decreases when porous parameter increased. The influence of gravitational parameter (η) on axial pressure gradient is presented in Fig. 10. Indeed, the axial pressure gradient is increases by increase in η (η = 0.1, 0.5, 1) with fixed Da = 0.3, β = 0.7, $\overline{Q} = \pi/6$, $\alpha = \pi/6$, M = 1, $\varepsilon = 0.2$, k1= 0.1, $t = \pi/4$, $\mu = 0.2$, d = 2. Fig.11. shows that the effect of inclined angle α on axial pressure gradient with fixed Da = 0.3, β = 0.7, $\phi = \pi/6$, $\eta = 0.5$, M = 1, $\varepsilon = 0.2$, k1= 0.1, $t = \pi/4$, $\overline{Q} = 0.2$, d = 2. We observe from this figure that the increasing the values of α (α = 0, π/6, π/3), the results in the flow field increases. Effect of volumetric flow rate ($\overline{Q}$) on axial pressure gradient is depicted in Fig. 12. We notice that the axial pressure gradient decreases by increasing the values of $\overline{Q}$ ($\overline{Q}$ = 0.2, 0.4, 0.6) with Da = 0.3, β = 0.7, $\phi = \pi/6$, $\alpha = \pi/6$, $\eta = 0.5$, M = 1, $\varepsilon = 0.2$, $k_1 = 0.1$, $t = \pi/4$, d = 2.

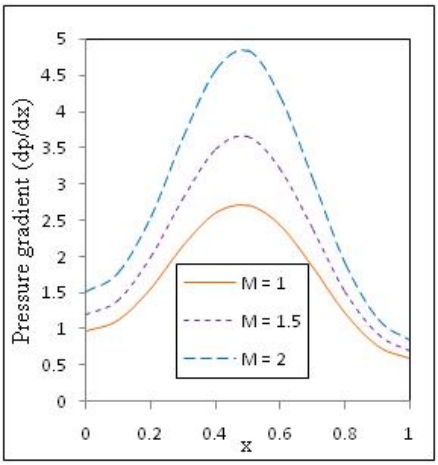

Figure (7): Pressure gradient (dp/dx) for different values of M with fixed Da = 0.3, $\phi = \pi/6$, $\alpha = \pi/6$, $\eta = 0.5$, $\beta = 0.7$, $\varepsilon = 0.2$, $k_1 = 0.1$, $t = \pi/4$, $\overline{Q} = 0.2$, d = 2.

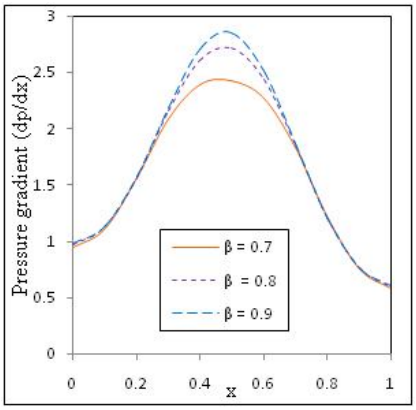

Figure (8): Pressure gradient (dp/dx) for different values of β with fixed M = 1, $\phi = \pi/6$, $\alpha = \pi/6$, $\eta = 0.5$, $\varepsilon = 0.2$, $k_1 = 0.1$, $t = \pi/4$, $\overline{Q} = 0.2$, d = 2.

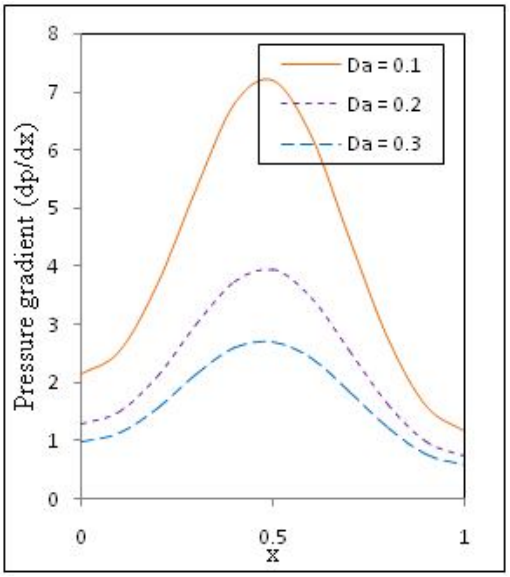

Figure (9): Pressure gradient (dp/dx) for different values of Da with fixed $\beta = 0.7$, $\phi = \pi/6$, $\alpha = \pi/6$, $\eta = 0.5$, $M = 1$, $\varepsilon = 0.2$, $k_1 = 0.1$, $t = \pi/4$, $\overline{Q} = 0.2$, $d = 2$.

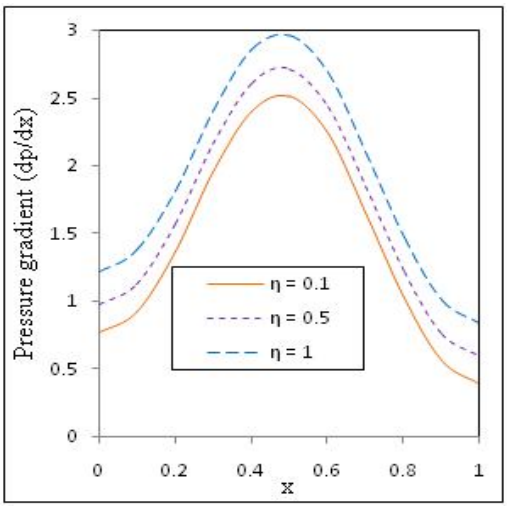

Figure (10): Pressure gradient (dp/dx) for different values of η with fixed $Da = 0.3$, $\beta = 0.7$, $\phi = \pi/6$, $\alpha = \pi/6$, $M = 1$, $\varepsilon = 0.2$, $k_1 = 0.1$, $t = \pi/4$, $\overline{Q} = 0.2$, $d = 2$.

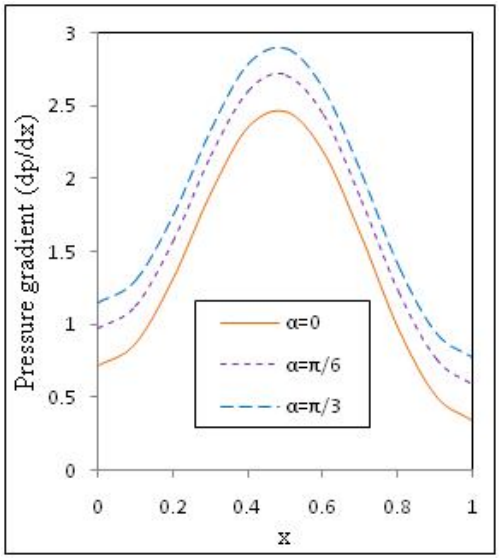

Figure (11): Pressure gradient (dp/dx) for different values of α with fixed $Da = 0.3$, $\beta = 0.7$, $\phi = \pi/6$, $\eta = 0.5$, $M = 1$, $\varepsilon = 0.2$, $k_1 = 0.1$, $t = \pi/4$, $\overline{Q} = 0.2$, $d = 2$.

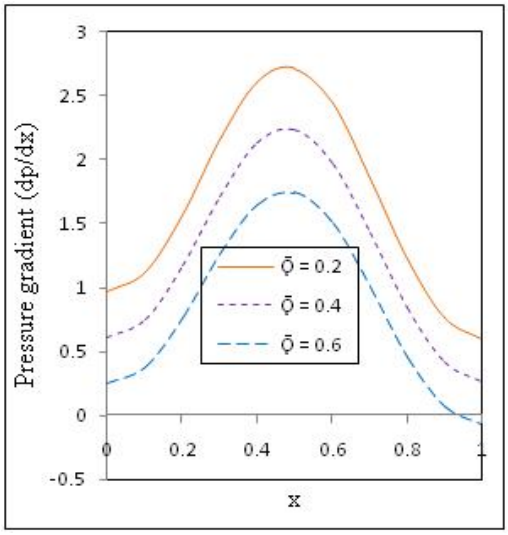

Figure (12): Pressure gradient (dp/dx) for different values of α with fixed $Da = 0.3$, $\beta = 0.7$, $\phi = \pi/6$, $\alpha = \pi/6$, $\eta = 0.5$, $M = 1$, $\varepsilon = 0.2$, $k_1 = 0.1$, $t = \pi/4$, $d = 2$.

Figure (13) shows that the temperature distribution (θ) for different values of Hartmann number increases (M = 1, 1.5, 2) with Da = 0.3, N = 0.5, Pr =1, γ = 0.1, Br = 0.1, ϕ = π/6, α = π/6, η = 0.5, β = 0.7, ε = 0.2, k_1= 0.1, x= 0.6, t = 0.4, p = 0.5. It was evident that the temperature distribution increases as increase in M. Figure (14) shows the variation slip parameter β (β = 0.7, 0.8, 0.9) on temperature (θ) with Da = 0.3, N = 0.5, Pr =1, γ = 0.1, Br = 0.1, M =1, ϕ = π/6, α = π/6, η = 0.5, ε = 0.2, k_1= 0.1, x= 0.6, t = 0.4, p = 0.5. It can be noticed that from this graph that the temperature of the fluid decreases due to increment in the slip parameter. Effect of porosity parameter Da (Da = 0.1, 0.2, 0.3) on temperature distribution (θ) is plotted in fig 15. We notice that the temperature distribution increases when increase in Da with fixed N = 0.5, Pr =1, γ = 0.1, Br = 0.1, M =1, ϕ = π/6, α = π/6, η = 0.5, β = 0.7, ε = 0.2, k_1= 0.1, x= 0.6, t = 0.4, p = 0.5. Fig. 16 reveals the different of radiation parameter N (N = 0.5, 0.7, 0.9) on temperature profile (θ) with Da = 0.3, Pr =1, γ = 0.1, Br = 0.1, M =1, ϕ = π/6, α = π/6, η = 0.5, β = 0.7, ε = 0.2, k_1= 0.1, x= 0.6, t = 0.4, p = 0.5. This figure indicates that the temperature distribution enhances when radiation parameter increased. Fig.17 presents the various values of Prandtl number Pr (Pr = 1, 3, 5) on temperature profile with fixed Da = 0.3, N =0.5, γ = 0.1, Br = 0.1, M =1, ϕ = π/6, α = π/6, η = 0.5, β = 0.7, ε = 0.2, k_1= 0.1, x= 0.6, t = 0.4, p = 0.5. It is obvious that the temperature distribution increases with increase in Prandtl number. Fig.18 depicts the temperature distribution (θ) with different values of Brinkman number Br (Br = 0.1, 0.2, 0.3) with Da = 0.3, Pr =1, N =0.5, γ = 0.1, M =1, ϕ = π/6, α = π/6, η = 0.5, β = 0.7, ε = 0.2, k_1= 0.1, x= 0.6, t = 0.4, p = 0.5. It was evident from the figure that the temperature distribution increases as increase in Br. The relation between temperature distribution (θ) and gravitational parameter (η) is shown in Fig. (19). It is clear that the temperature distribution decreases as η increases being fixed other parameters. Influence of various values heat source/sink parameter γ (γ = 0.1, 0.3, 0.5) on temperature distribution is presented in Fig.20 with fixed Da = 0.3, Pr =1, N =0.5, η = 0.5, M =1, ϕ = π/6, α = π/6, Br = 0.1, β = 0.7, ε = 0.2, k_1= 0.1, x= 0.6, t = 0.4, p = 0.5. This figure reveals that the temperature distribution increases as increase in γ.

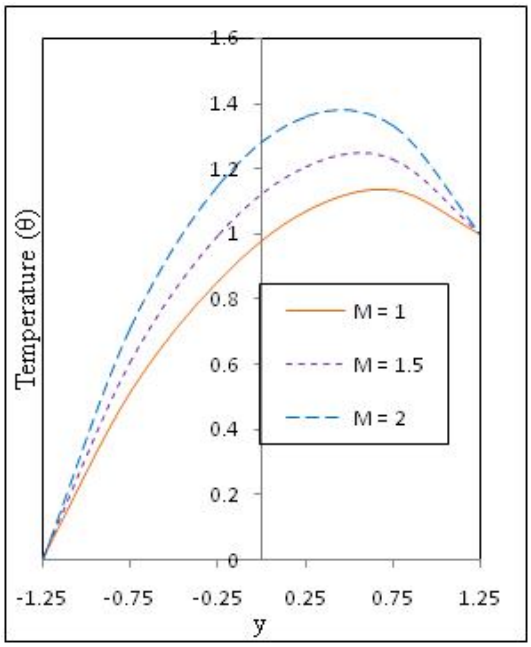

Figure (13): Temperature (θ) for different values of M with fixed Da = 0.3, N = 0.5, Pr =1, γ = 0.1, Br = 0.1, ϕ = π/6, α = π/6, η = 0.5, β = 0.7, ε = 0.2, k_1= 0.1, x= 0.6, t = 0.4, p = 0.5.

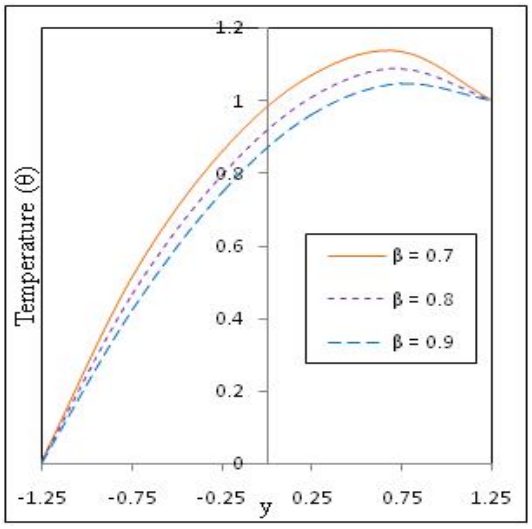

Figure (14): Temperature (θ) for different values of β with fixed Da = 0.3, N = 0.5, Pr =1, γ = 0.1, Br = 0.1, M =1, ϕ = π/6, α = π/6, η = 0.5, ε=0.2,k_1= 0.1, x= 0.6, t = 0.4, p = 0.5.

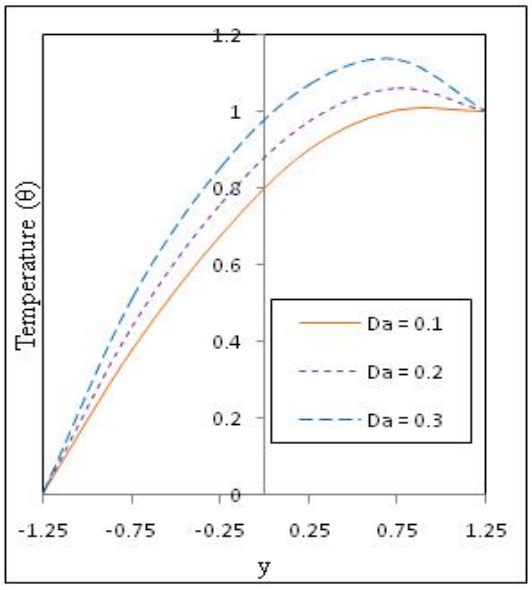

Figure (15): Temperature (θ) for different values of Da with fixed N = 0.5, Pr =1, γ = 0.1, Br = 0.1, M =1, ϕ = π/6, α = π/6, η = 0.5, β =0.7, ε=0.2, k_1= 0.1, x=0.6, t = 0.4, p= 0.5.

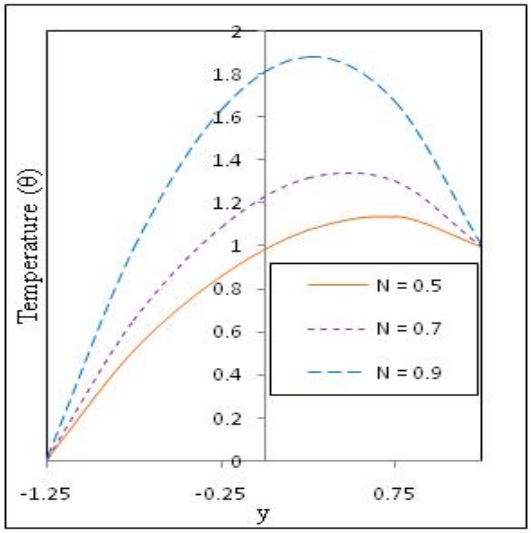

Figure (16): Temperature (θ) for different values of N with fixed Da = 0.3, Pr =1, γ = 0.1, Br = 0.1, M =1, ϕ = π/6, α = π/6, η = 0.5, β = 0.7, ε = 0.2, k_1= 0.1, x= 0.6, t = 0.4, p= 0.5.

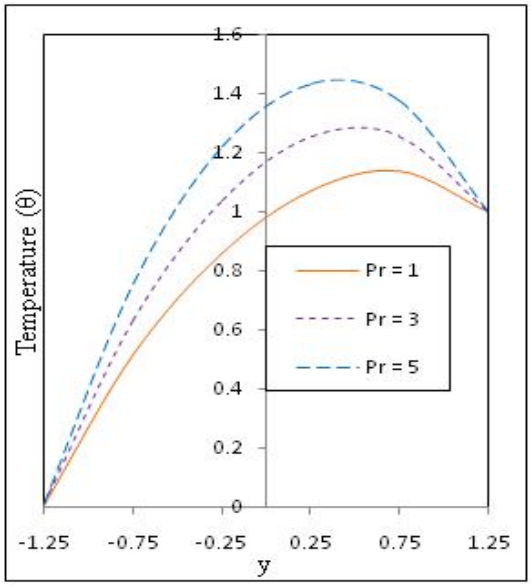

Figure (17): Temperature (θ) for different values of Pr with fixed Da = 0.3, N =0.5, γ = 0.1, Br = 0.1, M =1, ϕ = π/6, α = π/6, η = 0.5, β = 0.7, ε= 0.2, k_1= 0.1, x= 0.6, t = 0.4, p = 0.5.

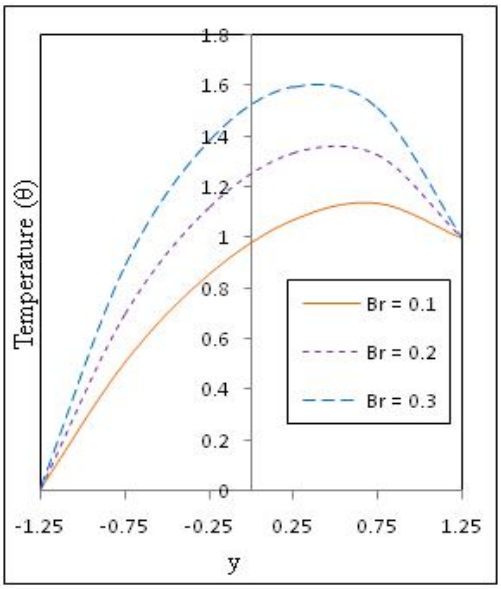

Figure (18): Temperature (θ) for different values of Br with fixed Da = 0.3, Pr =1, N =0.5, γ = 0.1, M =1, ϕ = π/6, α = π/6, η = 0.5, β = 0.7, ε = 0.2, k_1= 0.1, x= 0.6, t = 0.4, p = 0.5.

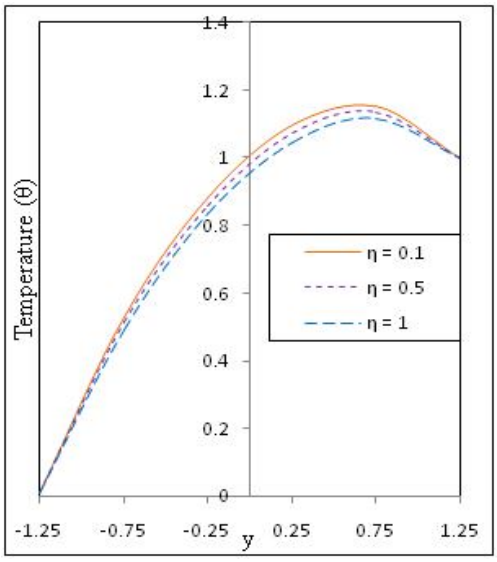

Figure (19): Temperature (θ) for different values of η with fixed Da = 0.3, Pr =1, N =0.5, M =1, ϕ = π/6, α = π/6, Br = 0.1, β = 0.7, η = 0.5, ε = 0.2, k_1= 0.1, x= 0.6, t = 0.4, p = 0.5.

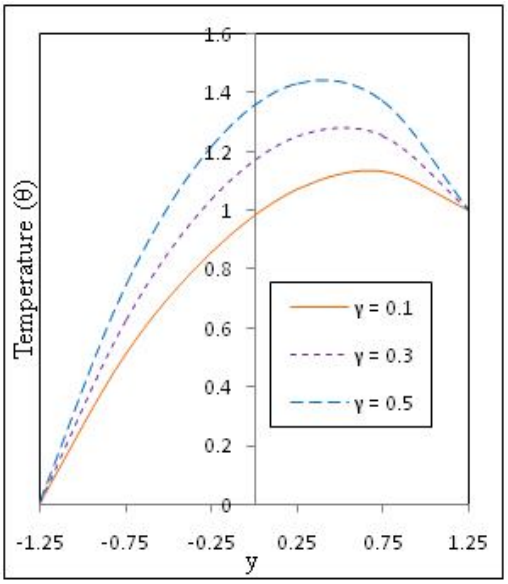

Figure (20): Temperature (θ) for different values of γ with fixed Da = 0.3, Pr =1, N =0.5, η = 0.5, M =1, ϕ = π/6, α = π/6, Br = 0.1, β = 0.7, ε = 0.2, k_1= 0.1, x= 0.6, t = 0.4, p = 0.5.

The influence of Hartmann number M on heat transfer coefficient at the wall y = h_1 is depicted in Fig. 21 with Da = 0.3, N = 0.5, Pr =1, γ = 0.1, Br = 0.1, ϕ = π/6, α = π/6, η = 0.5, β = 0.7, ε = 0.2, k_1= 0.1, t = 0.4, p= 0.5. It is obvious that the heat transfer coefficient increases in the portion of the inclined tapered channel x ε [0, 0.05] U [0.58, 1] and it is decreases in the other portion of the inclined tapered channel x ε [0.05, 0.58] with increase in M (M = 1, 1.5, 2). Fig. 22 presents the heat transfer coefficient with slip parameter being fixed Da = 0.3, M = 1, N = 0.5, Pr =1, γ = 0.1, Br = 0.1, ϕ = π/6, α = π/6, η = 0.5, ε = 0.2, k_1= 0.1, t = 0.4, p= 0.5.It was evident that from the graph that the heat transfer coefficient decreases in the portion of the inclined tapered channel x ε [0, 0.05] U [0.58, 1] and it is

increases in the other portion of the inclined tapered channel x ε [0.05, 0.58] as increase in β (β =0.7,0.8,0.9). Fig. 23 depicts the heat transfer coefficient at the wall y = h_1 for different values of porosity parameter Da (Da = 0.1, 0.2, 0.3) with M = 1, N = 0.5, Pr =1, γ = 0.1, Br = 0.1, β = 0.7, ϕ = π/6, α = π/6, η = 0.5, ε = 0.2, k_1= 0.1, t = 0.4, p= 0.5.It is clear that the heat transfer coefficient increases in the portion of the inclined tapered channel x ε [0, 0.05] U [0.58, 1] and it is decreases in the other portion of the inclined tapered channel x ε [0.05, 0.58] with increase in Da. The heat transfer coefficient at the wall y = $h_1$for various values of radiation parameter N (N = 0.5, 0.7, 0.9) is plotted in Fig. 24 with fixed M = 1, Da =0.3, Pr =1, γ = 0.1, Br = 0.1, β = 0.7, ϕ= π/6, α = π/6, η = 0.5, ε = 0.2, k_1= 0.1, t = 0.4, p= 0.5.We notice that the heat transfer coefficient increases in the portion of the channel x ε [0, 0.05] U [0.58, 1] and it is decreases in the other portion of the channel x ε [0.05, 0.58] with increase in N. The effect of Prandtl number Pr on heat transfer coefficient at the wall y = h_1 with M = 1, Da =0.3, N = 0.5, γ = 0.1, Br = 0.1, β = 0.7, ϕ = π/6, α = π/6, η = 0.5, ε = 0.2, k_1= 0.1, t = 0.4, p= 0.5 is shown in Fig.25.We observe that from this graph that the heat transfer coefficient increases in the portion of the channel x ε [0, 0.05] U [0.58, 1] and it is decreases in the rest of the channel x ε [0.05, 0.58] with increase in Pr (Pr = 1,3,5). Fig. 26 shows that the variation in heat transfer coefficient at the wall y = h_1 for different values of Brinkman number Br (Br = 0.1, 0.2, 0.3) with fixed M = 1, Da =0.3, N = 0.5, γ = 0.1, Pr = 1, β = 0.7, ϕ = π/6, α = π/6, η = 0.5, ε = 0.2, k_1= 0.1, t = 0.4, p= 0.5.We notice that the heat transfer coefficient increases in the portion of the channel x ε [0, 0.05] U [0.58, 1] and it is decreases in the rest of the channel x ε [0.05, 0.58] with increase in Br. Heat transfer coefficient at the wall y = h_1 for different values of gravitational parameter(η) with M = 1, Da =0.3, N = 0.5, γ = 0.1, Pr = 1, Br = 0.1, β = 0.7, ϕ = π/6, α = π/6, ε = 0.2, k_1= 0.1, t = 0.4, p= 0.5 as plotted in fig. 27. Indeed, the heat transfer coefficient decreases in the portion of the inclined tapered channel x ε [0, 0.05] U [0.58, 1] and it is increases in the other portion of the inclined tapered channel x ε [0.05, 0.58] as increase in η (η =0.1, 0.5, 1). The heat transfer coefficient at the wall y = h_1 for various values of heat source/sink parameter γ (γ = 0.1, 0.3, 0.5) is presented in Fig. 28 with M = 1, Da =0.3, N = 0.5, Pr = 1, Br = 0.1,β = 0.7, η = 0.5, ϕ = π/6, α = π/6, ε = 0.2, k_1= 0.1, t = 0.4, p= 0.5. It was evident that the heat transfer coefficient increases in the portion of the channel x ε [0, 0.05] U [0.58, 1] and it is decreases in the rest of the channel x ε [0.05, 0.58] as increase in increase in γ.

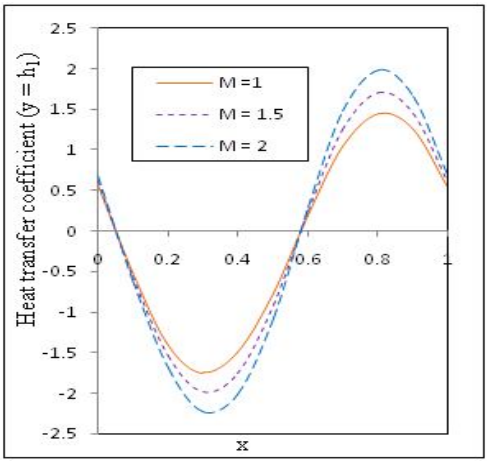

Figure (21): Heat transfer coefficient (y = h_1) for different values of M with fixed Da = 0.3, N = 0.5, Pr =1, γ = 0.1, Br = 0.1, ϕ = π/6, α = π/6, η = 0.5, β = 0.7, ε = 0.2, k_1= 0.1, t = 0.4, p= 0.5

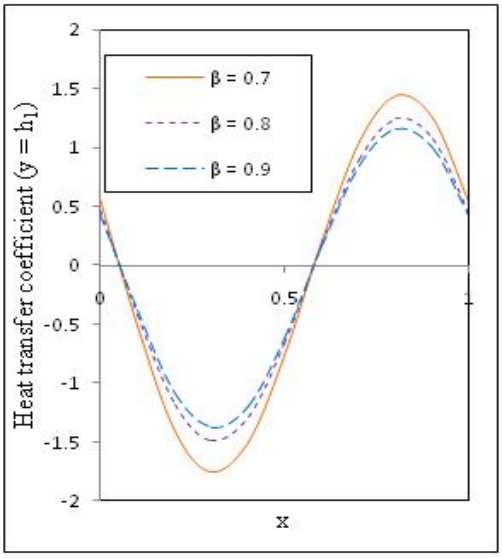

Figure (22): Heat transfer coefficient (y = h_1) for different values of β with fixed Da = 0.3, M = 1, N = 0.5, Pr =1, γ = 0.1, Br = 0.1, ϕ = π/6, α = π/6, η = 0.5, ε = 0.2, k_1 = 0.1, t = 0.4, p= 0.5

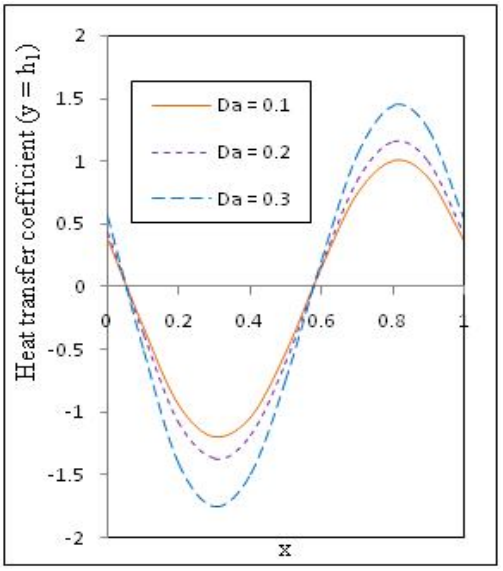

Figure (23): Heat transfer coefficient (y = h_1) for different values of Da with fixed M = 1, N = 0.5, Pr =1, γ = 0.1, Br = 0.1, β = 0.7, ϕ = π/6, α = π/6, η = 0.5, ε = 0.2, k_1 = 0.1, t = 0.4, p= 0.5

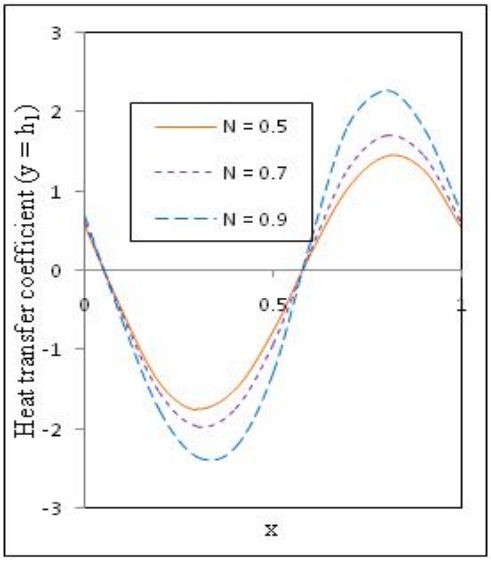

Figure (24): Heat transfer coefficient (y = h_1) for different values of N with fixed M = 1, Da =0.3, Pr =1, γ = 0.1, Br = 0.1, β = 0.7, ϕ = π/6, α = π/6, η = 0.5, ε = 0.2, k_1 = 0.1, t = 0.4, p= 0.5

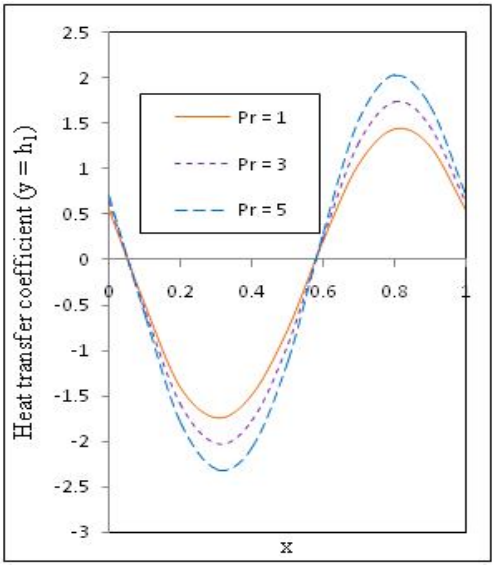

Figure (25): Heat transfer coefficient (y = h_1) for different values of Pr with fixed M = 1, Da =0.3, N = 0.5, γ = 0.1, Br = 0.1, β = 0.7, ϕ = π/6, α = π/6, η = 0.5, ε = 0.2, k_1 = 0.1, t = 0.4, p= 0.5

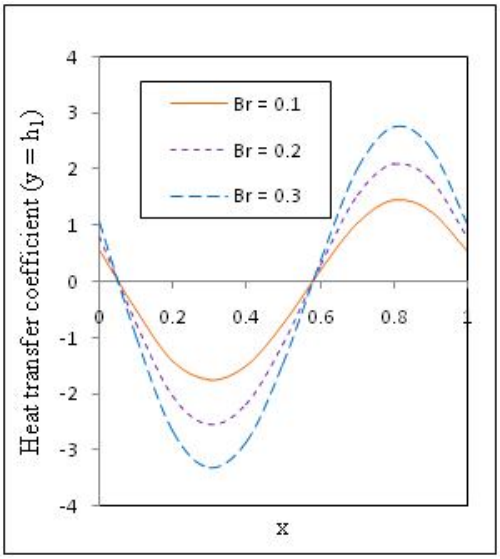

Figure (26): Heat transfer coefficient ($y = h_1$) for different values of Br with fixed M = 1, Da =0.3, N = 0.5, $\gamma = 0.1$, Pr = 1, $\beta = 0.7$, $\phi = \pi/6$, $\alpha = \pi/6$, $\eta = 0.5$, $\varepsilon = 0.2$, $k_1 = 0.1$, t = 0.4, p= 0.5

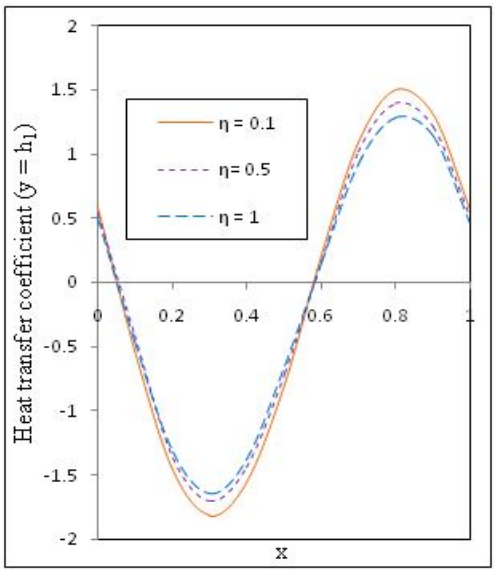

Figure (27): Heat transfer coefficient ($y = h_1$) for different values of η with fixed M = 1, Da =0.3, N = 0.5, $\gamma = 0.1$, Pr = 1, Br = 0.1, $\beta = 0.7$, $\phi = \pi/6$, $\alpha = \pi/6$, $\varepsilon = 0.2$, $k_1 = 0.1$, t = 0.4, p= 0.5

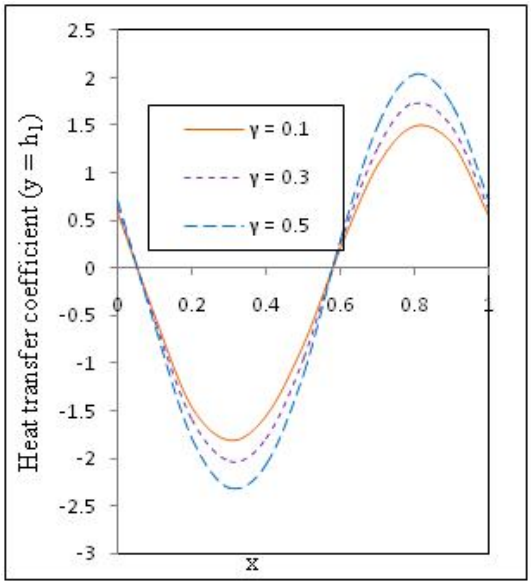

Figure (28): Heat transfer coefficient ($y = h_1$) for different values of γ with fixed M = 1, Da =0.3, N = 0.5, Pr = 1, Br = 0.1, $\beta = 0.7$, $\eta = 0.5$, $\phi = \pi/6$, $\alpha = \pi/6$, $\varepsilon = 0.2$, $k_1 = 0.1$, t = 0.4, p= 0.5

Conclusions

An influence of slip and joule heating on MHD peristaltic blood flow with uniform porous medium through an inclined asymmetric vertical tapered channel in the presence of radiation -blood flow model. The important findings of the present study are summarized below.

(1) Axial velocity increases with increase in M, β, η and α.
(2) Axial velocity decreases with increase in Da.
(3) Pressure gradient enhances with increase in M, β, η and α.
(4) Pressure gradient decreases with increase in porous parameter (Da) and Volumetric

flow rate ($\overline{Q}$).

(5) Temperature distribution increases with increase in M, Pr, Da, N, α and Br.

(6) Temperature distribution decreases with increase in β and η.

(7) Heat transfer coefficient increases in the portion of the inclined tapered channel x ε [0, 0.05] U [0.58, 1] and it is decreases in the other portion of the inclined tapered channel x ε [0.05, 0.58] with increase in M, Pr, Da, N, γ and Br

References

1. Abzal, S.K., Vijaja Kumar Varma, S. and Ravikumar, S. Influence of heat transfer on magnetohydrodynamic peristaltic blood flow with porous medium through a coaxial vertical asymmetric tapered channel - an analysis of blood flow study. International Journal of Engineering Sciences & Research Technology, vol.*5* (4), pp. 896-915(2016).
2. Cogley, A.C.L., Vinvent, W.G. and E.S. Giles, E.S. Differential approximation for radiative heat transfer in non-linear equations-grey gas near equilibrium. American Institute of Aeronautics and Astronautics, vol. *6,* pp. 551–553(1968).
3. Fung, Y.C. and Yih, C.S. Peristaltic Transport. *J. Appl. Mech., 35*, pp.669-675 (1968).
4. Hayat, T., Abbasi, F. M. and Alsaedi, A. Soret and Dufour effects on peristaltic flow in an asymmetric channel. *Arab J Sci Eng, 39*, pp. 4341–4349(2014).
5. Hayat, T., Rija Iqbal, Anum Tanveer and Ahmed Alsaedi. Influence of convective conditions in radiative peristaltic flow of pseudoplastic nanofluid in a tapered asymmetric channel. Journal of Magnetism and Magnetic Materials, *408*,168-176 (2016).
6. Hayat, T, Qureshi, M.U. and Ali, N. The influence of slip on the peristaltic motion of a third order fluid in an asymmetric channel. PhysLett A, Vol. *372*, 2653–2664 (2008).
7. Kawang-Hua Chu, W. and Fang, J. Peristaltic transport in a slip flow. European Physical Journal B, 16, pp. 543-547(2000).
8. Kothandapani, M., Pushparaj, V. and Prakash, J. On Effects of Slip and Heat Transfer on the MHD Peristaltic Flow of a Jeffery Fluid through a Vertical Tapered Asymmetric Channel, Global Journal of Pure and Applied Mathematics (GJPAM) ISSN 0973-1768 Volume *12*, Number 1, pp. 205-212 (2016).
9. Kothandapani, M. and Srinivas, S. On the influence of wall properties in the MHD peristaltic transport with heat transfer and porous medium. Phy. Lett. A, 372, pp. 4586–4591 (2008).
10. Krishna Kumari, S.V.H.N., M.V. Ramana Murthy, M. V., Ravi Kumar, Y.V.K. and Sreenadh, S. Peristaltic Pumping of a Jeffrey Fluid under the Effect of Magnetic Field in an Inclined Channel. Applied Mathematical Sciences, Vol. *5*, no. 9, and pp. 447 – 458 (2011).
11. Kumar, M. A., Sreenadh, S., Saravana, R., Reddy, R.H. and Kavitha, A. Influence of velocity slip conditions on MHD peristaltic flow of a Prandtl fluid in anon-uniform channel, Malaysian Journal of Mathematical Sciences *10(1):* 35–47

(2016).

12. Latham, T.W. 1966. Fluid Motion in a Peristaltic Pump. MSc Thesis, Massachusetts Institute of Technology, Cambridge, Massachusetts.
13. Lika Hummady and Ahmed Abdulhadi. Influence of MHD on Peristaltic Flow of Couple-Stress Fluid through a Porous Medium with Slip Effect. Advances in Physics Theories and Applications, Vol. *30*, pp. 34-44 (2014).
14. Mishra, M. and Rao, A.R. Peristaltic transport of a Newtonian fluid in an asymmetric channel. Z. Angew Math. Phys., *54*, pp. 440-532 (2004).
15. Mustafa, M., Abbasbandy, S., Hina, S. and Hayat, T. Numerical investigation on mixed convective peristaltic flow of fourth grade fluid with Dufour and Soret effects. J Taiwan Institute of Chemical Engineers, *45*, pp. 308–316 (2014).
16. Nadeem, S., Hayat, T., Akbar, N. S. and Malik, M.Y. On the influence of heat transfer in peristalsis with variable viscosity. Int. J. Heat Mass Transfer, 52, pp. 4722–4730 (2009).
17. Ramana Kumari, A.V. and G. Radhakrishnamacharya, G. Effect of slip on peristaltic transport in an inclined channel with wall effects,Int. J. of Appl. Math and Mech., *7* (1), pp. 1-14 (2011).
18. Ravikumar, S. Analysis of Heat Transfer on MHD Peristaltic Blood Flow with Porous Medium through Coaxial Vertical Tapered Asymmetric Channel with Radiation – Blood Flow Study. International Journal of Bio-Science and Bio-Technology Vol.*8*, No.2, pp.395-408 (2016).
19. Ravikumar, S. Ahmed, A. Magnetohydrodynamic couple Stress Peristaltic flow of blood Through Porous medium in a Flexible Channel at low Reynolds number. Online International Interdisciplinary Research Journal, vol. III, no. VI, pp. 157-166 (2013).
20. Ravikumar, S. and Siva Prasad, R. 2010. Interaction of pulsatile flow on the peristaltic motion of couple stress fluid through porous medium in a flexible channel. Eur. J. Pure Appl. Math, vol. 3, pp. 213-226.
21. Ravikumar, S. Hydromagnetic Peristaltic Flow of Blood with Effect of Porous Medium through coaxial vertical Channel: A Theoretical Study .International Journal of Engineering Sciences & Research Technology, vol. 2, no. 10, pp. 2863-2871 (2013).
22. Ravikumar, S. Effect of couple stress fluid flow on magnetohydrodynamic peristaltic blood flow with porous medium trough inclined channel in the presence of slip effect-Blood flow study. International Journal of Bio-Science and Bio-Technology, vol. *7*, No. 5, pp.65-84 (2015).
23. Ravikumar, S. Effects of the couple stress fluid flow on the magnetohydrodynamic peristaltic motion with a uniform porous medium in the presence of slip effect. Jordan Journal of Mechanical and Industrial Engineering (JJMIE), vol.*9*, No. 4, pp. 269– 278 (2015).
24. Reddy, R.H., Kavitha1, A., Sreenadh, S. and Saravana, R. Effect of induced magnetic

field on peristaltic transport of a carreau fluid in an inclined channel filled with porous material,International Journal of Mechanical and Materials Engineering (IJMME), Vol. *6,* No.2, pp. 240-249 (2011).

25. Shapiro, A.M., Jaffrin, M.Y. and Weinberg, S. L. Peristaltic pumping with long wavelength at low Reynolds number. Jour Fluid Mech., *37*, pp.799-825 (1969).
26. Shehzad, S.A., Abbasi, F.M., Hayat, T. and Alsaadi, F. MHD Mixed Convective Peristaltic Motion of Nanofluid with Joule Heating and Thermophoresis Effects. PLoS ONE, 9(11), e111417 (2014).
27. Srinivas, S. and Pushparaj, V. Non-linear peristaltic transport in an inclined asymmetric channel. Communications in Nonlinear Science and Numerical Simulation, *13*, pp. 1782–1795 (2008).
28. Vajravelu, K., Radhakrishnamacharya, G. and Radhakrishnamurty, V. Peristaltic flow and heat transfer in a vertical porous annulus with long wave approximation. *Int. J. Nonlinear Mech., 42*, pp. 754–759 (2007).
29. Venugopal Reddy, K. and Gnaneswara Reddy, M. Velocity slip and joule heating effects on MHD peristaltic flow in a porous medium. *Int. J. Adv. Appl. Math. And Mech., 2(2),* pp. 126 – 138(2014).